The severity factor as a useful tool for producing hydrochars and derived carbon materials

Asma Jeder, Angela Sanchez-Sanchez, Philippe Gadonneix, Eric Masson, Abdelmottaleb Ouederni, Alain Celzard, Vanessa Fierro

The severity factor as a useful tool for producing hydrochars and derived carbon materials

Asma Jeder[1,2], Angela Sanchez-Sanchez[1], Philippe Gadonneix[1], Eric Masson[3], Abdelmottaleb Ouederni[2], Alain Celzard[1], Vanessa Fierro[1*]

1 Institut Jean Lamour, UMR Université de Lorraine - CNRS 7198, ENSTIB, 27 rue Philippe Séguin, BP 21042, 88051 Epinal cedex 9, France

2 Laboratory of Research: Process Engineering and Industrial Systems ($LR_{11}ES_{54}$), National School of Engineers of Gabès, University of Gabès, 6026 Gabès, Tunisia

3 Crittbois, 27 rue Philippe Seguin, BP 91067, 88051 Epinal Cedex 9, France

[*]Corresponding author. Tel: + 33 372 74 96 77. Fax: + 33 372 74 96 38
E-mail address : Vanessa.Fierro@univ-lorraine.fr (V. Fierro)

Abstract

The main purpose of this study was to understand the effect of time and temperature during the hydrothermal carbonisation (HTC) of olive stones (OS). For that purpose, the severity factor was introduced, by which the effect of the HTC conditions on the resultant products could be described. HTC was carried out at various temperatures (160, 180, 200, 220 and 240°C) and times (3, 6, 12, 24 and 48 hours) for producing 25 hydrochars. The yield to hydrochar varied from 70 to 50%. Hydrochars were all submitted to thermogravimetric and elemental analysis. The liquid fractions were also recovered and analysed in order to valorise OS as completely as possible. Thus, highly added-value products such as furfural and 5-hydroxymethylfurfural were detected. At the highest temperature and time, the hydrochar elemental composition was similar to that of lignite coals. Hydrochars were further carbonised at 900°C, leading to materials with surface areas as high as 1200 m^2 g^{-1} and with narrow pore size distributions centred on 0.5 nm. The severity factor allowed finding clear tendencies in the production of hydrochars and derived carbons in terms of yield, composition, and surface area, which would have been hardly analysed if the effects of temperature and time had to be considered separately. We proved that the severity factor, which use is quite uncommon in studies dealing with materials production, is a valuable tool for studying the effects of HTC experimental conditions.

Keywords: biomass valorisation; olive stones; hydrothermal carbonisation; severity factor; carbon; furfural; 5-hydroxymethylfurfural.

1. Introduction

Olive production holds a strategic position in Tunisia economy. The Tunisian olive groves include over 65 million trees and the olive production in 2015 was around 1.4 million tons, according to the Tunisian Ministry of Agriculture. Olive stones (OS) are by-products of olive oil extraction, and are burnt for heating and cooking in domestic applications or are used for energy co-generation in industry. Lately, OS have been considered as an attractive agriculture residue in applications related to energy and environment (Bhatnagar et al. 2014; Bohli et al. 2015; Ghouma et al. 2015). OS composition depends on oil extraction methods and drying but is mainly composed of lignin, cellulose and hemicellulose. In Tunisia, olive oil is produced by traditional pressing, so that OS have high moisture content (Pattara et al. 2010).

As OS are widely available by-products in Tunisia and in other Mediterranean countries, abundant research has been done to valorise them with possible applications in different industrial sectors such as petrochemistry (Ubago-Pérez et al. 2006), electrochemistry (Tejeda-Ricardez et al. 2003) cosmetics (Mohammadi et al. 2010) and pharmacology (Martínez et al. 2006). OS pyrolysis was thoroughly studied as a way to produce activated carbon (Javad Hosseini et al. 2012; Díaz et al. 2013; Bhatnagar et al. 2014). Acid hydrolysis of OS has also been studied to produce furfural in hydrothermal conditions (Montané 2002; Román et al. 2013; Borrero-López et al. 2016) studied the hydrothermal carbonisation (HTC) of OS and concluded that hydrochars prepared from OS were more reactive towards air and CO_2 activation than chars obtained by traditional OS pyrolysis. They concluded that HTC can play a very important role in the future production of tailored activated carbons for particular applications such as adsorption, electrochemical or gas storage, and catalysis.

In a previous study (Borrero-López et al. 2016), the possibility of producing high added-value products, mainly furfural (FU) and 5-hydroxymethylfurfural (5-HMF) on the one hand, and hydrochars and carbons on the other hand, was evaluated. FU production yield up to 19.9%, based on the hemicellulose content, was obtained. Other minor, but valuable, compounds such as 5-HMF and some phenolic compounds were also produced. One hydrochar was carbonised at 900°C and the resultant carbon material was highly ultramicroporous with a peak of pore size distribution centred on 0.5 nm, and a high surface areas around 1000 m^2 g^{-1}, typical of most carbon molecular sieves. (Borrero-López et al. 2016) used low HTC times because the objective was to produce FU and 5-HMF. The highest FU yield was obtained at short times (4 and 6 h) and moderate temperatures (180 and 190°C), whereas the highest yield of 5- HMF was achieved in the most severe conditions considered in that work (240°C, 2 h).

The objective of the present study was to go deeper in the analysis of the solid fraction obtained after HTC of OS, and in the possibility of using OS as precursor of carbon materials. For that purpose, we studied the effects of much broader ranges of time (3, 6, 12, 24, 48 h) and temperature (160, 180, 200, 220 and 240°C) on the physicochemical characteristics of the hydrochars and of the derived carbon materials. Previous studies were carried out on the optimisation of char production from palm shell (Nizamuddin et al. 2016), olive stone (Álvarez-Murillo et al. 2015), tomato peel (Sabio et al. 2016) or wood (Sermyagina et al. 2015; Gao et al. 2016) among others biomasses (Nizamuddin et al. 2017), concluding that temperature and time were the most important variables. In the present study, time and temperature were combined by using the severity factor, a quite uncommon parameter when it comes to the preparation of materials but which allowed establishing clear trends. The analysis of the thermogravimetric curves of cellulose, hemicellulose, lignin and hydrochars also provided information about the effect of temperature and time during the

hydrothermal treatment of OS. The resultant carbon materials presented a microporous nature with a high faction of narrow micropores centred on 0.5 nm, and surface areas as high as 1270 m^2 g^{-1}.

2. Experimental

2.1 Raw material

Olive stones (OS) were obtained from a local factory in Gabès, Tunisia. They were ground to a particle size lower than 1 mm, and thoroughly washed with hot distilled water. The OS were then dried at 105°C for 24 h prior to analysis. Alpha-cellulose and lignin contents were determined according to T203 and T222 Tappi standards, respectively. Hemicellulose was determined by difference. Lignin, cellulose and hemicellulose contents in OS were found to be 29.88, 40.53 and 21.68 wt. %, respectively, as already reported elsewhere (Borrero-López et al. 2016).The content of hot-water extractives from olive stone was determined using the T264 Tappi standard method. Holocellulose was extracted according to the method of Wise et al. (Wise et al. 1946).

2.2 Hydrochar and carbon synthesis

2 g of ground OS were mixed with 16 mL of distilled water and placed in a glass flask, itself introduced in a 100 mL Teflon®-lined autoclave for hydrothermal carbonisation (HTC).The autoclaves were hermetically closed and installed into a preheated oven at a defined temperature (160, 180, 200, 220 or 240°C) and for a defined time (3, 6, 12, 24 or 48h).Temperature and time are the most important variables in liquid hot water treatments. The reaction ordinate, R_0, based on the combination of temperature, T (°C), and residence time, t (min), was defined by (Overend et al. 1987) to describe the impact of liquid hot water treatments on lignocellulosic components:

$$R_0 = t \cdot \exp\left(\frac{T-100}{14.75}\right) \quad (1)$$

In Eq. (1), 14.75 is the activation energy (kJ mol^{-1}) based on the assumptions that the reaction is hydrolytic and the overall conversion is first-order. The logarithm of the reaction ordinate, (log R_0), was defined at the severity of the hydrothermal carbonisation, i.e., the severity factor.

The pressure inside the reactor was auto-generated by the water evaporated at the set point in the limited volume of the autoclave. After the reaction time, the autoclave was removed from the oven and cooled down to room temperature for several hours. The solids recovered after HTC, i.e., the hydrochars, were separated from the remaining liquid phase by filtration, and then washed with distilled water and dried in an oven at 80°C for 8 hours. The hydrochar yield was defined as the ratio of the weights of hydrochar to initial OS, on dry basis.

Hydrochars were subsequently carbonised in a quartz tube installed in a tubular furnace, which was heated at 1°C min^{-1} up to 900°C under nitrogen flow. The final temperature was maintained for 3 h, after which the samples were cooled under nitrogen flow. Next, the carbon materials were recovered and weighed after drying at 105°C for 24h. The carbonisation yield was calculated as the mass ratio of carbon material to hydrochar, on dry basis. The total yield to carbon was calculated as the mass ratio of final carbon material to raw OS, again on dry basis.

2.3 Characterisation

Elemental analysis of samples was carried out in an Elementar EL Cube apparatus for determining carbon, nitrogen, hydrogen, and sulphur contents. Oxygen content was obtained by difference.

Pore texture characteristics were determined by physical adsorption of CO_2 and N_2 at -196°C and 0°C, respectively, using an ASAP 2020 automatic manometric analyser (Micromeritics, USA). Each sample was degassed for at least 24h at 250°C. Due to the narrow porosity and the long diffusion times of N_2 at -196°C, only six selected carbons were analysed by N_2 adsorption. The surface area was calculated by applying the Brunauer-Emmett-Teller (BET) and the 2-D Non-Linear Density Functional Theory - Heterogeneous Surface (NLDFT-HS) (Jagiello and Olivier 2013) models to the CO_2 adsorption branch of the isotherms, leading to values of $A_{BET,CO2}$ and $S_{NLDFT,CO2}$, respectively. For those carbons analysed by both N_2 and CO_2 adsorption, the pore size distributions (PSDs) were determined by application of the Saieus® software version 2.02 provided by Micromeritics (Jagiello et al. 2015). The total S_{NLDFT} for each carbon was calculated by addition of the $S_{NLDFT,\ CO2}$ and the $S_{NLDFT,\ N2}$.

Thermogravimetric analyses (TGA) were performed using a STA 449F1 apparatus (Netzsch, Germany). In a typical experiment, 40 mg of sample were loaded into an alumina crucible and heated at 10°C min^{-1} from room temperature to 900°C under an argon flow of 20 mL min^{-1}. Weight and temperature were continuously recorded along the experiment. TGA were carried out on hydrochars and compounds separated from OS: lignin, holocellulose and alpha-cellulose.

Selected liquid samples after HTC were separated and investigated using a Clarus 500 GC gas chromatograph (Perkin-Elmer Inc., USA) coupled to a Clarus 500 MS quadrupole mass spectrometer (Perkin-Elmer Inc., USA). Samples were analysed after liquid-liquid extraction using the following procedure. In a screw-capped vial, 5 mL of dichloromethane were added to 1 mL of hydrothermal liquid, and the resultant solution was stirred vigorously. Next, the dichloromethane phase was removed from the solution and then analysed by GC-MS as such or after derivatisation, i.e., as trimethyl derivatives. The latter were obtained as

follows. In a screw-capped vial, 0.4 mL of N,O-bis-(trimethylsilyl) trifluoroacetamide containing 1% of trimethylchlorosilane and 0.1 mL of pyridine were added to 0.5 mL of extract. The solution was stirred and heated at 80°C for 30 min. After evaporation of the solvent in a stream of dry nitrogen, the residue was diluted in 1 mL of dichloromethane.

3. Results and discussion

3.1 Characteristics of olive stones

The hot water extractives content were found to represent 7.9 wt. % of the dry OS. These compounds usually include fats, free sugar and phenolic compounds (Rodríguez et al. 2008). Such amount is consistent with values reported in the literature for biomass containing 35 to 50 % of lignin, and in which the cellulose content is higher than that of hemicellulose (Nefzaoui 1991; Blanco López et al. 2002). Elemental analysis showed that the present OS had the typical following mass composition: carbon, 50.10 wt. %; oxygen, 43.50 wt. %; hydrogen, 6.22 wt. %; nitrogen, 0.15 wt. %; sulphur, 0.04 wt. %.

Figure 1(a) shows the differential TGA curves of OS. Three major weight losses were observed: a first one between 60 and 160°C, corresponding to the evolution of moisture, a second one between 215 and 310°C, and a third one between 310 and 360°C with a maximum weight loss of 47% at around 340°C. At temperatures higher than 360°C and up to approximately 700°C, a steady weight loss was observed (Figure S1 of the Electronic Supplementary Information) that might be attributed to the very progressive charring of the material. In order to correctly interpret these thermogravimetric results, alpha-cellulose, cellulose and lignin were investigated separately and the corresponding differential TGA curves are shown in Figure 1(b), 1(c) and 1(d), respectively. Figure 1(b) shows that alpha-cellulose degradation starts at 200°C and ends at 400°C with a maximum at 320°C. Figure

1(c) shows the thermal decomposition of holocellulose, with a maximum at 320°C and a shoulder at 270°C. Since holocellulose is cellulose plus hemicellulose, the shoulder was attributed to the degradation of hemicelluloses. Finally, Figure 1(d) corresponds to lignin, whose decomposition takes place in a broader range of temperature from 200 to 800°C, in good agreement with the results reported by other authors (Fierro et al. 2005). Therefore, the long decomposition tail observed up to 800°C is probably due to lignin, which represents 29.88 wt. % of OS, and the 2nd and 3rd weight losses of OS can be mainly attributed to the decomposition of hemicellulose and alpha-cellulose, respectively.

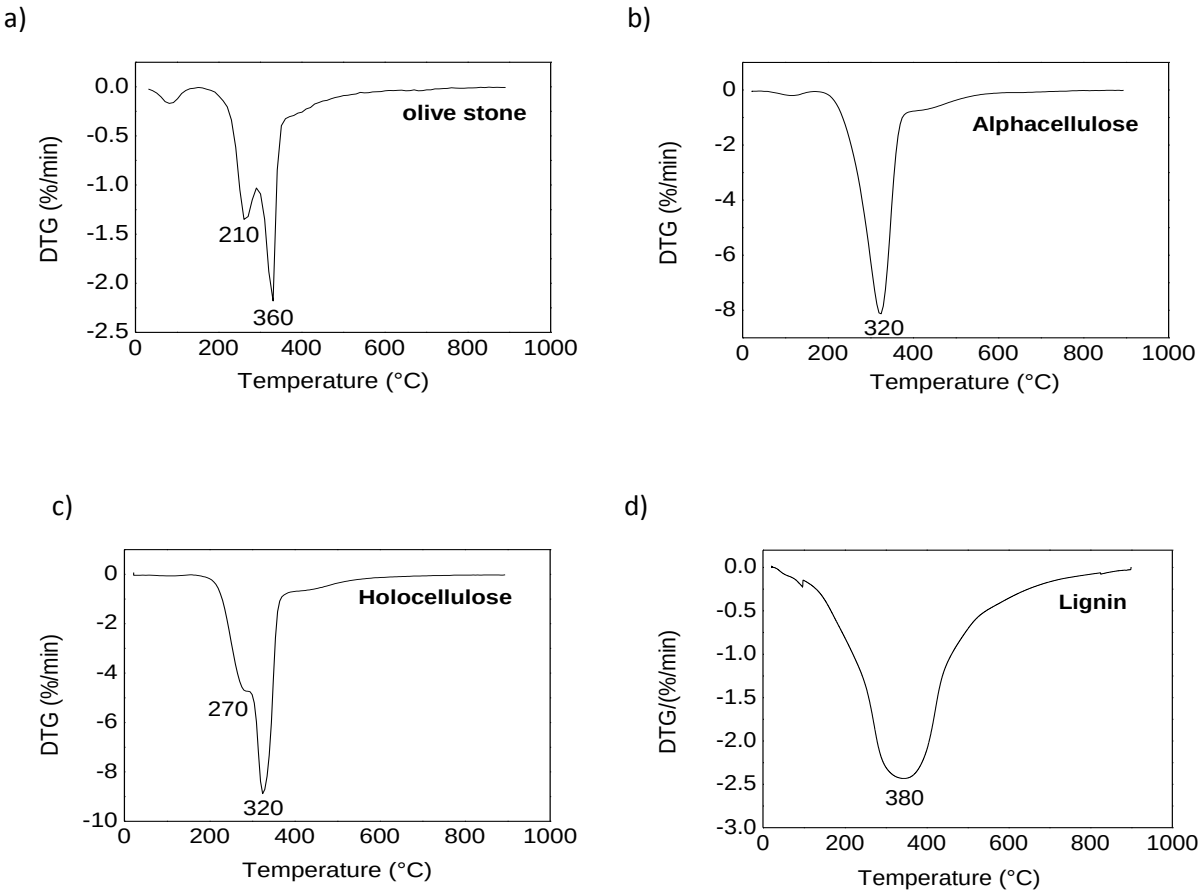

Fig. 1. Differential TGA curves of: a) olive stone, and of its main compounds: b) alpha-cellulose, c) holocellulose, and d) lignin.

3.2 Characteristics of OS-based hydrochars

Figure 2(a) shows the changes of hydrochar yield as a function of time, at various HTC temperatures. The yield varied from 70 % (160°C, 3h) to 50 % (240°C, 24h). In this figure, the discontinuous lines are only guides for the eye; the decrease of yield can be easily observed when time and temperature increase. Hydrochar yields were slightly higher than those reported for OS by Alvarez-Murillo et al. (Álvarez-Murillo et al. 2015) and similar to those obtained from olive tree trimmings (OT) and olive pulp (OP) (Volpe and Fiori 2017). The latter finding might appear surprising as OT and OP have higher hemicellulose and cellulose contents than OS, but OT and OP were submitted to HTC for only 0.5h. Hydrochar yields from OS were also much higher than those obtained from eucalyptus bark (Gao et al. 2016), corn stalk (Guo et al. 2015), microalgae (Heilmann et al. 2010) or palm shell (Nizamuddin et al. 2016) at similar HTC severities; this is due to the high lignin content of OS. In order to represent the effects of both parameters at the same time, the hydrochar yield was plotted in Figure 2(b) as a function of severity factor (log R_0, see Eq. (1)). The severity factor varied from 4.0 to 7.6 and easily allowed observing a direct relationship between the hydrochar yield and the combined effect of temperature and time. This decrease of yield was accompanied by carbon enrichment and related decreases of oxygen and hydrogen contents.

Figure 2(c) thus shows the inverse relationship between the O/C atomic ratio and the severity factor. Cellulose and hemicellulose hydrolysis indeed produces a loss of oxygen and hydrogen and the corresponding enrichment in carbon of the hydrochars (Parshetti et al. 2013). Figure 2(d) shows the van Krevelen diagram for the hydrochars prepared in this study. The H/C and O/C atomic ratios of OS were given as a reference (see the full black hexagon in this Figure), and are equal to 1.49 and 0.65, respectively. Dehydration (H_2O loss) and decarboxylation (CO_2 loss) reactions during HTC also produced some changes in the elemental composition of OS-derived hydrochars (Wiedner et al. 2013). At low severity of 4

(160°C, 3 and 6 h), the composition of the hydrochar (H/C = 1.48; O/C = 0.60) was similar to that of pristine OS. At the highest severity, 7.58, a significant change in the hydrochar elemental composition was observed (H/C = 0.87; O/C = 0.27). The latter values are similar to those of lignite coals (H/C = 0.9; O/C = 0.2) (Benavente et al. 2015).

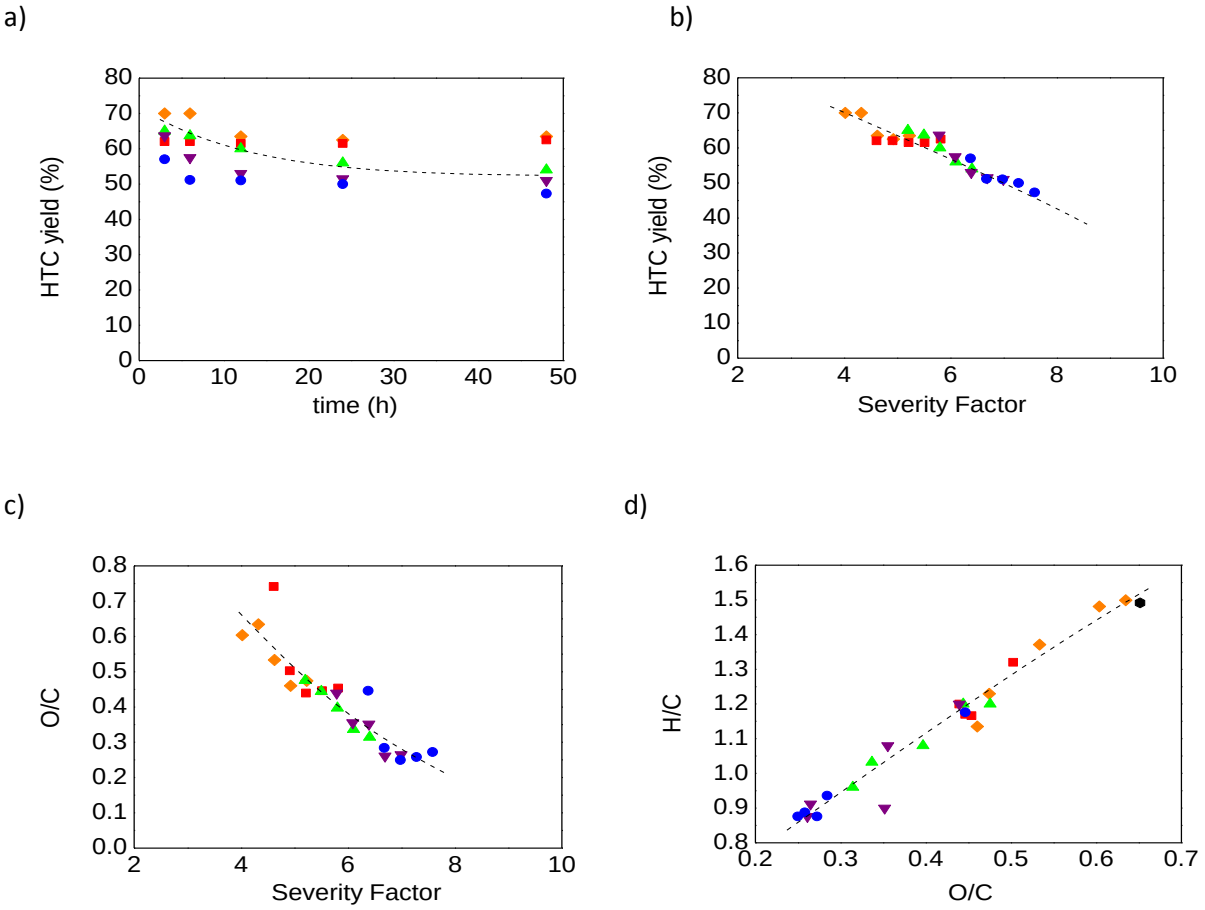

Fig. 2. Hydrochar yield as a function of: (a) time, and (b) severity at different temperatures. c) Variation of the O/C ratio with the severity; d) Van Krevelen diagram of the hydrochars. (◆ T=160°C, ■ T=180°C, ▲ T =200°C, ▼ T =220°C, ● T=240°C, ● Direct pyrolysis)

Hydrochars are commonly used: (i) for soil amendment with multiple environmental benefits: reducing soil nutrient leaching losses, reducing bioavailability of environmental contaminants, sequestering carbon, reducing greenhouse gas emissions, and enhancing crop productivity in highly weathered or degraded soils (Ippolito et al. 2012); (ii) as a source of

energy (Kambo 2014; Álvarez-Murillo et al. 2015; Reza et al. 2016); or (iii) as precursor of carbon materials (Hu et al. 2010; Braghiroli et al. 2015; Sánchez-Sánchez et al. 2016). The latter application has been studied herein.

In order to get insight into the mechanisms taking place during HTC, the resultant hydrochars were submitted to thermogravimetric analysis. The thermal behaviour of biomass during HTC is highly related to the treatment conditions such as time and temperature. Figure 3 shows the differential TGA results for hydrochars produced at temperatures ranging from 160°C (Figure 3(a)) to 240°C (Figure 3(e)). The corresponding curves were characterised by the absence of hemicelluloses peak such as those observed at 210°C in Figure 1(a) or at 270°C in Figure 1(c), which means that hemicellulose was hydrolysed at temperatures lower than 160°C. According to (Peterson et al. 2008), hemicellulose is easily dissolved in water at temperatures above 180°C and, moreover, the pressure auto-generated in the present study should also favour hemicellulose dissolution and hydrolysis. (Mok and Antal Jr 1993) found that it is possible to extract an average of 95% of hemicellulose as monomeric sugars working at 200-230°C within a few minutes only. Reza (Reza 2011) reported that most of hemicellulose is extracted, and likely hydrolysed to monosaccharides at 200°C in 5 min. In the present study, OS treated at 160°C for 3 h presented roughly the same differential TGA curve as that of OS treated at 180°C for 3h. Therefore, hemicellulose from OS can be hydrolysed at temperatures as low as 160°C, provided that the HTC lasts for at least 3h.

Figure 3(b) shows the differential TGA curves of hydrochars obtained at various HTC times at 180°C. The peak appearing at 380°C disappeared progressively when the HTC time increased from 3 to 48h. When increasing the temperature, the peak was shifted towards higher temperatures and was attributed to lignin, which is the most stable of the three considered biopolymers. Some authors even considered that lignin is an inert compound during HTC (Reza 2011). However, increasing the severity may significantly alter the three-

dimensional structure of lignin. (Jin 2014) reported that biomass conversion can be controlled by water density, which reflects water changes at the molecular level such as solvation effect, hydrogen bonding, polarity, dielectric strength, molecular diffusivity and viscosity. Kanetake (Kanetake et al. 2007) found that the decomposition of lignin was enhanced by increasing water density.

When biomass is submitted to HTC, several parallel and sequential reactions occur. In order to draw some conclusions about the effect of HTC severity on the reactions taking place, 5 ranges of temperatures were identified in which maxima of weight loss appeared: T1 (260-300°C), T2 (325-340°C), T3 (360-365°C), T4 (400-425°C), and T5 (475-560°C). Each differential TGA curve was then deconvoluted using Gaussian functions with the Origin® software, and each area corresponding to the aforementioned ranges of temperature was divided by the total area of the peaks. The value of each area normalised by the total area was then plotted for each HTC time and temperature, and the results are given in Figure S2 of the Electronic Supplementary Information. Figure 3(f) shows the area fraction, i.e., the ratio of peak area to total peaks area × 100, of each temperature range as a function of the severity factor. It can be seen that hydrochars decomposed at higher temperatures when the HTC severity increased.

The area fraction corresponding to the temperature range 260-300°C was the lowest at low severity but still existed at severity as high as 7.5. The contributions of the second (325-340°C) and the third 360-365°C) temperature ranges almost disappeared at severity factors higher than 6 and might correspond to the total transformation of cellulose. The same results were observed with rye straw (Titirici 2013), confirming the existence of a temperature threshold in which fibrous networks of cellulose disrupt when submitted to hydrothermal carbonisation. (Kumagai and Hirajima 2014) reported that hydrolysis is enhanced at temperatures close to 250°C because hot compressed water has a dissociation constant about

three orders of magnitude higher than that of water in ambient conditions; in this case, water acts as an acid–base catalyst precursor (Kruse and Dinjus 2007).

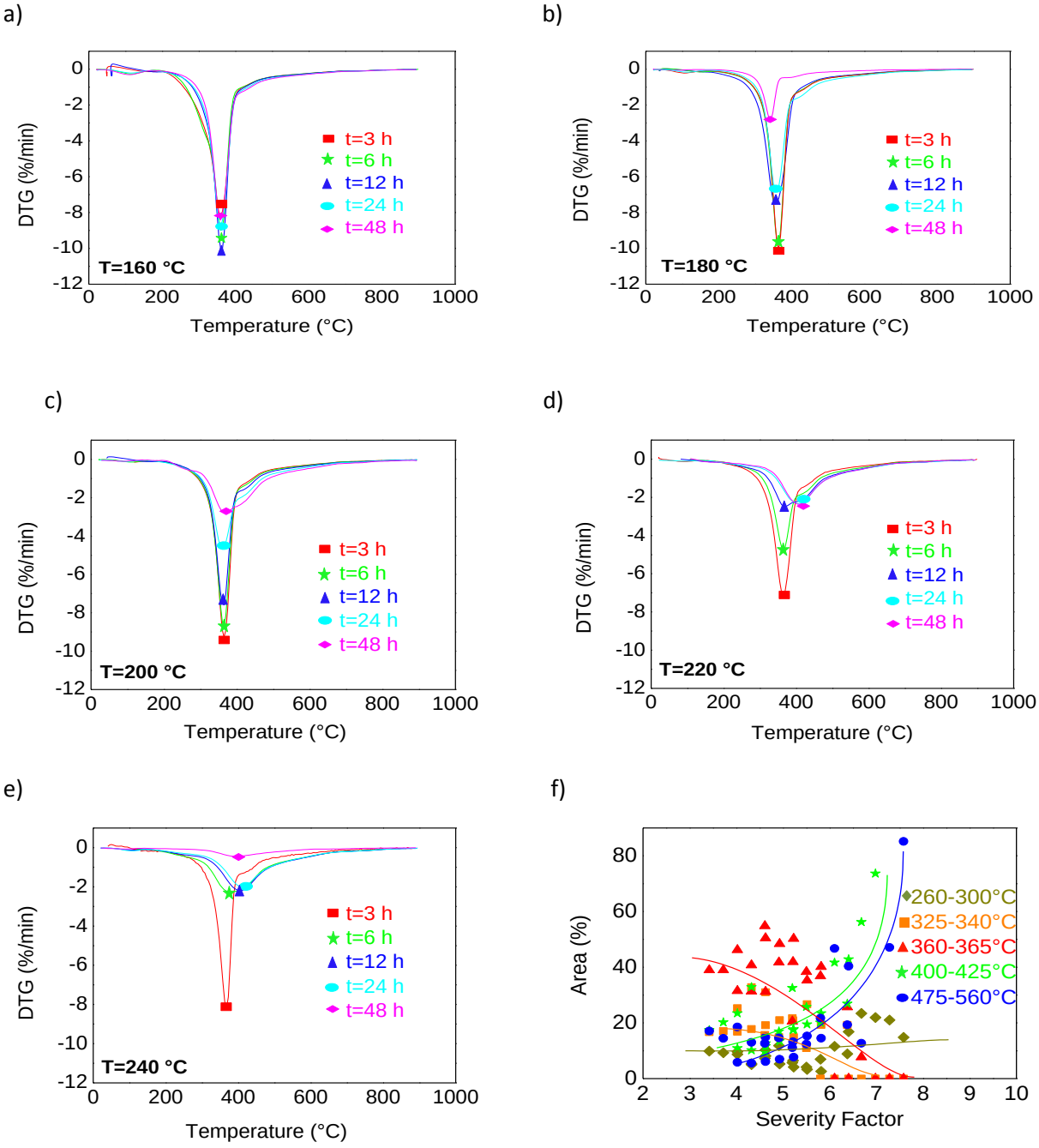

Fig. 3**:** (a) to (e) Differential TGA curves of hydrochars synthesised at temperatures ranging from 180 to 240°C and at reactions times ranging from 6 to 48h; (f) fraction of peak areas as a function of severity factor.

Thermal decomposition at the two final temperature ranges (400-425°C and 475-560°C) was especially important at severity factors higher than 5 (220°C and 24 h), and corresponds to the fraction of lignin that was not degraded at lower severity.

3.3 Characteristics of carbon materials

The 25 hydrochars were carbonised at 900°C under nitrogen atmosphere to produce carbon materials whose main characteristics were examined in order to evaluate their potential applications.

3.3.1 Carbon yield and elemental composition

Figure 4(a) and 4(b) present the carbonisation yield and the total yield, respectively. The latter was calculated as the hydrochar yield multiplied by the carbonisation yield. The carbonisation yield varied from 59 and 26 %, and hence the total yield to carbon materials varied from 28 to 16%.The latter might seem to be low while using OS as carbon precursor, but it should be recalled that a previous HTC step was carried out. The total yield was 28% when using the highest severity factor, 7.58. The higher carbonisation and total yields observed at higher severity factor might be due to the enhanced evolution of oxidising gases, especially CO_2 and H_2O. These gases can indeed oxidise and thus gasify carbon during pyrolysis, thereby reducing the carbon yield. Moreover, hydrochars were more aromatic and hence more stable when increasing the severity factor. OS directly submitted to pyrolysis for the sake of comparison had a carbonisation yield of 28%. Therefore, a preliminary HTC step at the highest severity (i.e., 7.58) before carbonisation did not modify the total yield to carbon when compared with direct pyrolysis, but allowed recovering a valuable liquid fraction and a carbon with a more aromatic structure and a more developed pore texture, as it will be shown below.

Figure 4(b) shows the Van Krevelen diagram of the carbon materials. The relationship between H/C and O/C was not linear. Unlike hydrochars, for which a linear relationship between H/C and O/C was found (see again Figure 2(d)) because HTC is governed by dehydration and decarboxylation, while carbonisation is generally governed by decarboxylation reactions (Oliveira et al. 2013).

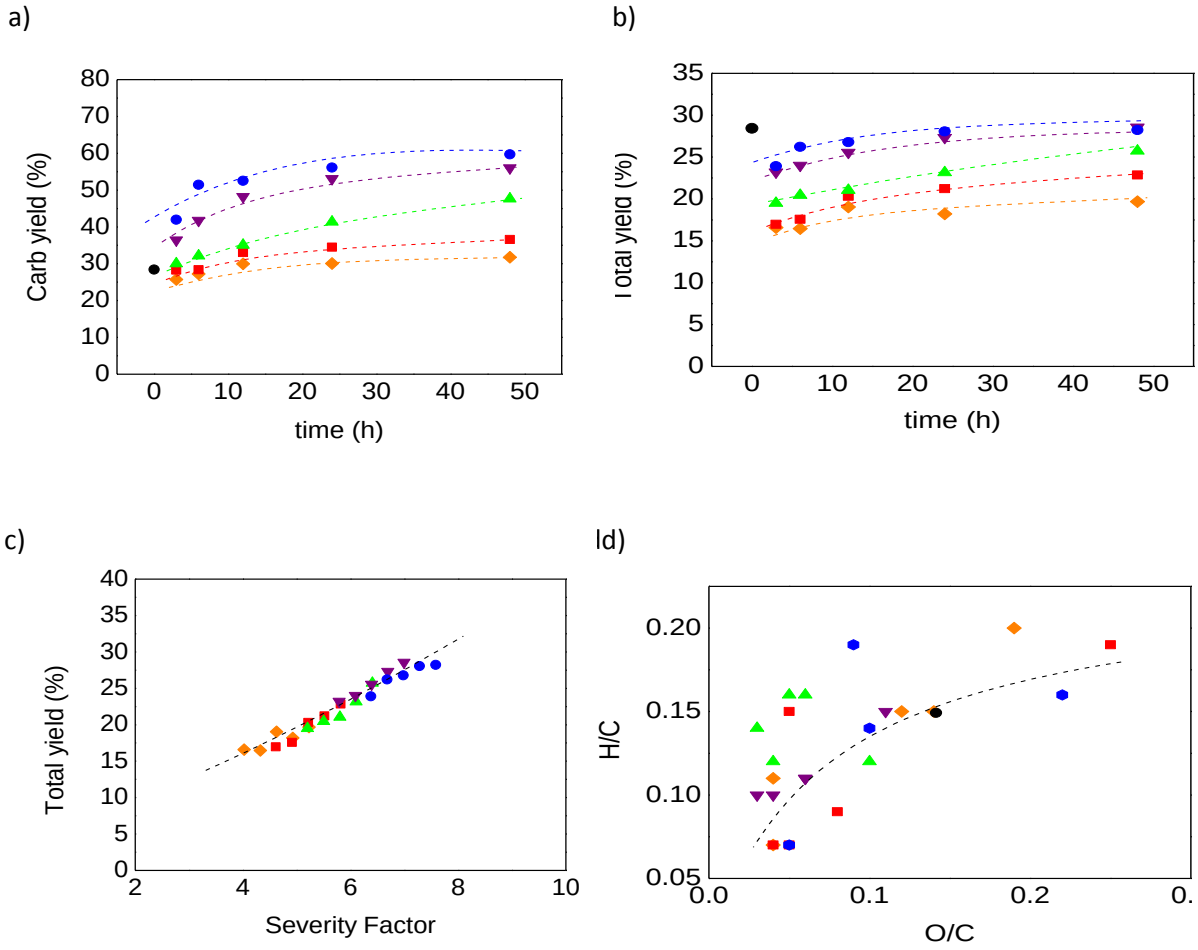

Fig. 4. (a) Carbonisation yield of hydrochars as a function of HTC time; (b) Total yield of the same, as a function of HTC time; (c) Total yield as a function of severity factor; (d) Van Krevelen diagram of carbonised hydrochars (◆ T=160°C, ■ T=180°C, ▲ T =200°C, ▼ T =220°C, ● T=240°C, ● Direct pyrolysis)

3.3.2 Porous texture

Nitrogen and carbon dioxide adsorption are powerful techniques providing detailed information about the textural properties of solids: pore volumes, pore size distributions and

surface areas. However, using N_2 as adsorbate at -196°C may be problematic for characterising very narrow micropores because diffusion of nitrogen is quite slow at such low temperature. As a consequence, the analyses are not only extremely long but, most of the time, are erroneous (Rodriguez-Reinoso et al. 1989). CO_2 is therefore recommended as a suitable mean for the complete determination of textural parameters of porous solids (Lowell et al. 2012) because it allows the assessment of pores narrower than 1 nm. In the present case, and although CO_2 diffusion is known to be much faster than that of N_2, the experiments lasted 7-10 days, suggesting the presence of extremely narrow pores. Six selected samples, chosen to cover the complete range of severities used in this study, were analysed by both N_2 and CO_2 adsorption.

Figure 5(a) shows the $S_{NLDFT,CO2}$ surface area as a function of HTC temperature and time. There was no clear trend with temperature, but a decrease the surface area with time can be observed. Figure 5(b) shows $S_{NLDFT,CO2}$ and $A_{BET,CO2}$ surface areas as a function of severity factor: $S_{NLDFT,CO2}$ varied from 662 to 942 $m^2\ g^{-1}$ while $A_{BET,CO2}$ varied between 320 and 446 $m^2\ g^{-1}$. Similar results were obtained by (Román et al. 2013) by CO_2 activation of a hydrochar synthesised using OS submitted to HTC at 220°C for 20 hours (A_{BET} = 438 $m^2\ g^{-1}$), and such surface area was higher than that obtained by air activation (A_{BET} = 204 $m^2\ g^{-1}$). Figure 5(c) shows $S_{NLDFT,CO2}$ as a function of $A_{BET,CO2}$. $S_{NLDFT,CO2}$ was always two times higher than $A_{BET,CO2}$. The BET model indeed assumes that a monolayer of CO_2 is adsorbed on pore walls and uses the cross-sectional area of CO_2 for calculating the surface area. But in the case of very narrow pores, the real surface is underestimated (divided by a factor 2) because only one CO_2 monolayer can fit between two very near pore walls(Do et al. 2010). Figure 5(d) shows the variation of the total pore volume determined by CO_2 adsorption, $V_{NLDFT,CO2}$, as a function of severity. The volume of narrow pores (i.e., < 1 nm) determined by CO_2 decreased with

increasing severity. This finding may be explained by pore widening and by the progressive degradation of lignin during HTC, as discussed below.

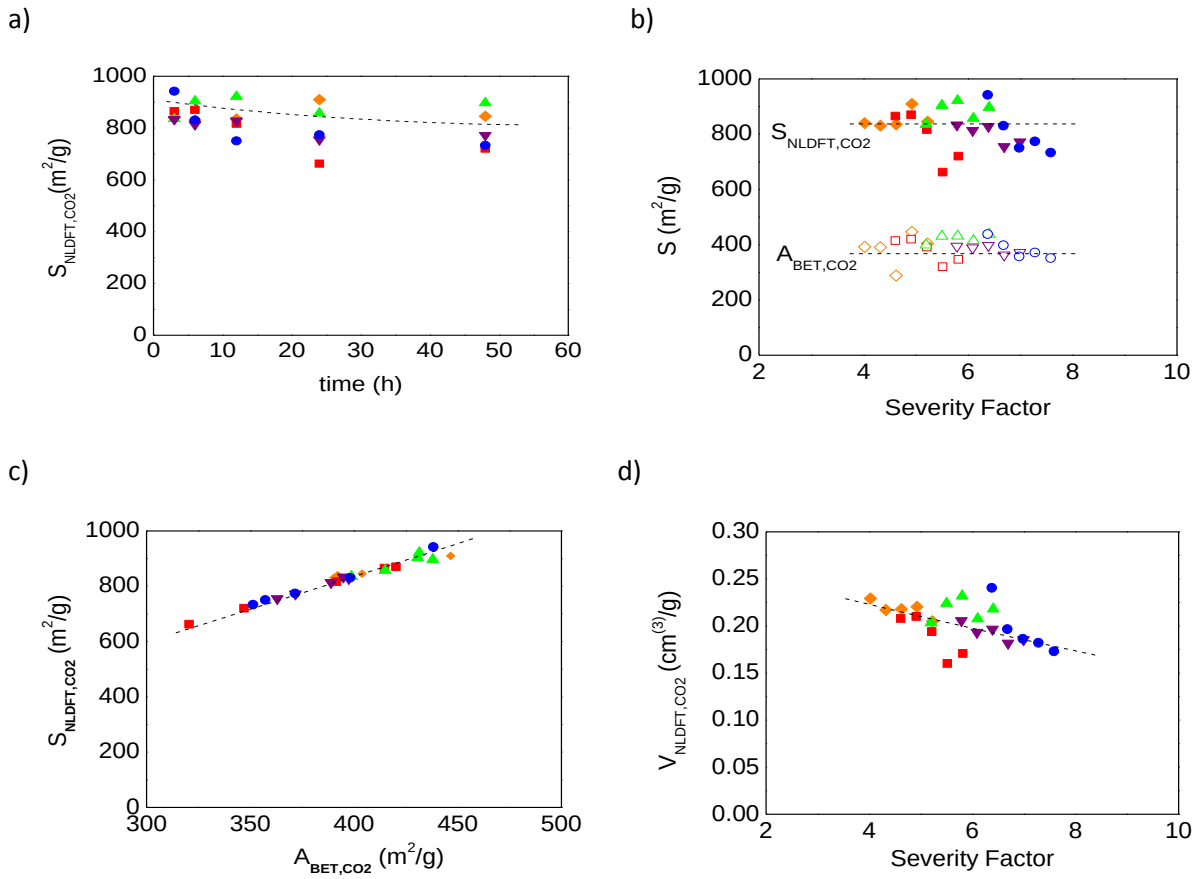

Fig. 5. Surface areas of hydrochar-derived carbons: (a) $S_{NLDFT,CO2}$ as a function of HTC time; (b)$S_{NLDFT,CO2}$ (full symbols) and $A_{BET,CO2}$ (empty symbols) as a function of severity; (c) $S_{NLDFT,\ CO2}$ as a function of $A_{BET,CO2}$; (d) Pore volume $V_{NLDFT,CO2}$ as a function of severity factor. (◆ T=160°C, ■ T=180°C, ▲ T =200°C, ▼ T =220°C, ● T=240°C)

6 selected carbons out of the 25 ones prepared in this work were analysed by both N_2 and CO_2 adsorption in order to have a complete overview of the textural properties of these materials. Figures 6(a) to 6(c) show the pore size distributions (PSDs) calculated when applying the NLDFT-HS model to the CO_2 and N_2 isotherms for carbons prepared at severities equal to 4.3, 6.1 and 7.3. On the one hand, PSDs obtained from CO_2 isotherms, thus corresponding to the narrower porosity, did not vary significantly. On the other hand, PSDs obtained from N_2 adsorption significantly changed with the HTC severity. At a

severity of 4.3, the maximum of the PSD was centred on 0.6 nm and the maximum was much less sharp than the one derived from CO_2 adsorption, which means that CO_2 could probe a much narrower microporosity than N_2. Increasing the severity of the HTC up to a severity of 6.1 further increased the height of the peak of the PSD, but the maximum remained at 0.6 nm. This means that the average pore width was similar but the amount of pores increased. Finally, at a severity of 7.3, the maximum was shifted to 0.7 nm and the PSD was broader. The application of the Saieus® software to obtain a unique PSD and S_{NLDFT} value from both isotherms, N_2 and CO_2, (Jagiello et al. 2015) gave illogical results, as the corresponding surface area was much lower than that obtained only from the CO_2 isotherm. Therefore, the S_{NLDFT} was calculated by taking into account $S_{NLDFT,\ CO2}$ and $S_{NLDFT,N2}$, using $S_{NLDFT,\ CO2}$ up to the point of intersection between both PSDs, around 0.6-0.7 nm, and $S_{NLDFT,N2}$ above the latter pore width. Figures 6(a) to 6(c) also show the cumulated S_{NLDFT} surface areas as function of pore width. Finally, Figure 6(d) shows the changes of S_{NLDFT} with the HTC severity. S_{NLDFT} varied from 800 to 1270 $m^2\ g^{-1}$ at severities ranging from 4.3 to 4.9, respectively. In fact, surface areas were around 800 $m^2\ g^{-1}$ for both the lowest and highest severities, whereas carbons prepared from hydrochars obtained at intermediate HTC severities presented a surface area around 1250 $m^2\ g^{-1}$. Such a feature, associated with the very narrow PSDs centred on 0.6 nm, makes these materials be potential cheap carbon molecular sieve. Increasing severity, cellulose was progressively degraded and the porosity and the surface area of the resultant carbon were higher, attaining the weak maximum shown in Figure 6(d). When the severity was higher than 6.5, lignin, whose pyrolysis fundamentally produces microporous carbons (Suhas et al. 2007), started to be modified, see Figure 3(d). More gases evolved during pyrolysis, producing the broadening of the PSD and, therefore, the S_{NLDFT} decreased. Further development of the porosity could be carried out by physical or chemical activation in order to produce activated carbons (ACs)

with wider PSDs, higher average pore sizes and an enhanced surface functionality (Jain et al. 2016; Tan et al. 2017). Thus, hydrochars have been activated with KOH (Schaefer et al. 2016) to obtain activated carbons with surface areas as high as 2240 m^2 g^{-1}, and were used for hydrogen storage.

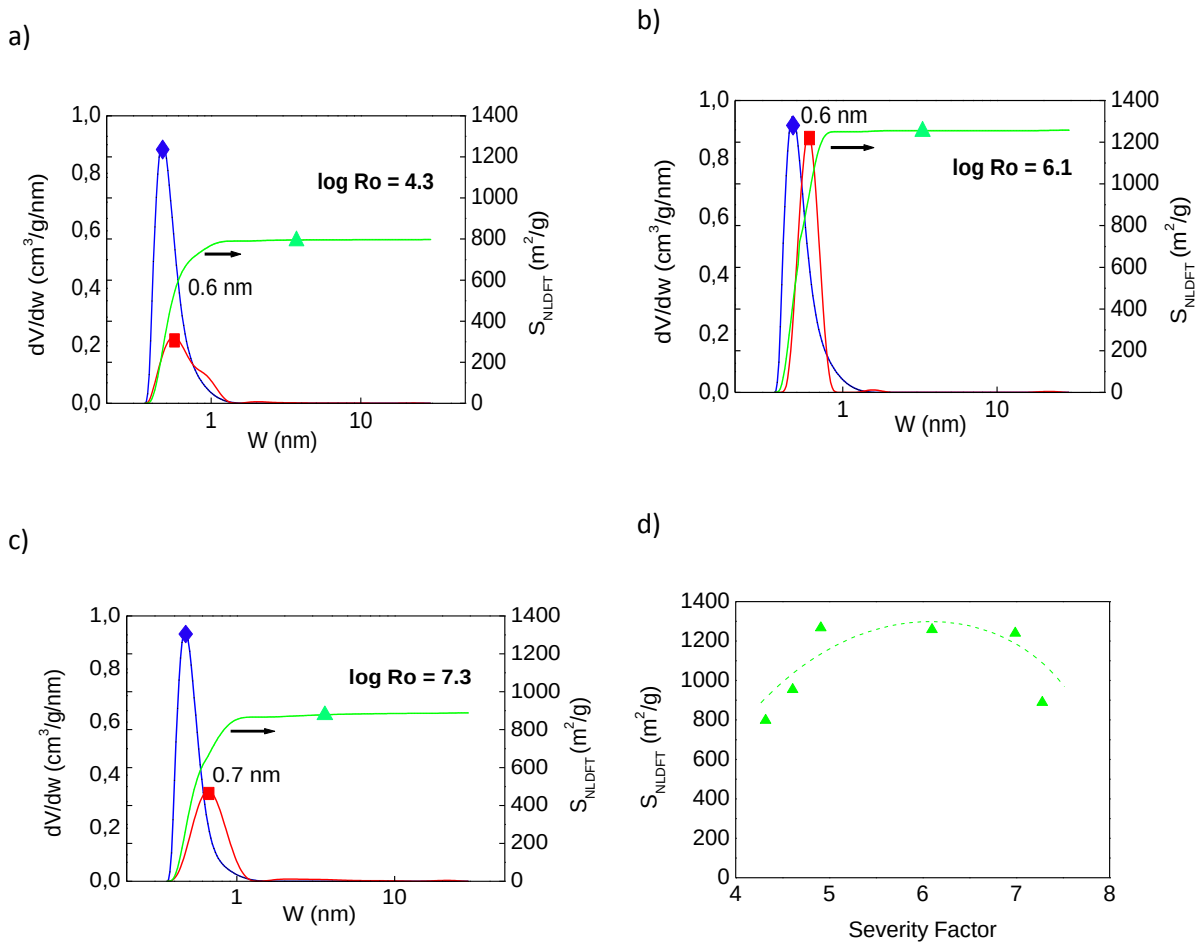

Fig. 6.NLDFTpore size distributions, CO_2 (◆) and N_2 (■), and S_{NLDFT} (▲) of carbons derived from hydrochar prepared at severity of: (a) 4.3 (160°C, 6h); (b) 6.1 (200°C, 24h); and (c) 7.3 (240°C, 24h); d) S_{NLDFT} (▲) versus severity (discontinuous line is a guide for the eye).

3.4 Liquid fraction

The liquid fraction recovered after HTC of OS was rich in valuable organic molecules such as FU, 5-HMF and organic acids. Figures 7(a) and 7(b) show the GC-MS analysis of two liquid fractions obtained at severities of 4.6 and 6.4, respectively. At severity 4.6, FU (7.30 min) and HMF (9.12 min) were the major compounds. FU is the result of hemicelluloses degradation and is classified as one of the top added-value chemicals (Anthonia and Philip 2015) as it can be used as selective solvent in the refining of lubricating oils, as gasoline additive, or as decolourising agent. FU production from OS was optimised in a former study, leading to a maximum of 19.9 % based on hemicellulose content of OS (Borrero-López et al. 2016). The liquid fraction also contained 5-HMF, which is mainly formed by the decomposition of cellulose. 5-HMF is also a versatile, multifunctional product that can be used as an intermediate in the synthesis of polymers (Yang et al. 2011). For instance, 5-HMF is used in the production of bioplastics, which are potential substitutes to petroleum-derived plastics commonly used in beverage bottles. Even at a severity of 4.2, aldehydes were observed, such as vanillin (17.60 min) and 4-hydroxy-3-methoxycinamaldehyde (22.96 min), coming from the decomposition of lignin. FU and 5-HMF remained present in the liquid fraction until a severity of 6.10.

Figure 7(b) shows the organic molecules present in the liquid fraction at a severity of 6.40 (T=200°C, t=48h): FU and 5-HMF totally disappeared. This result confirms the former TGA conclusions, according to which cellulose degradation submitted to HTC starts at low severity and is completed at 6.69. The GC-MS studies primarily showed organic molecules derived from lignin degradation such as vanillin (17.55 min), 1-(4-hydroxy-3-methoxyphenyl)-2-propanone (19.63 min) and 1-(2,4,6-Trihydrixypenyl)-2-pentanone (23.22 min). These compounds are of significant importance for producing a broad range of fine chemicals, particularly aromatic compounds, as well as fuel additives (Zhang et al. 2008).

a)

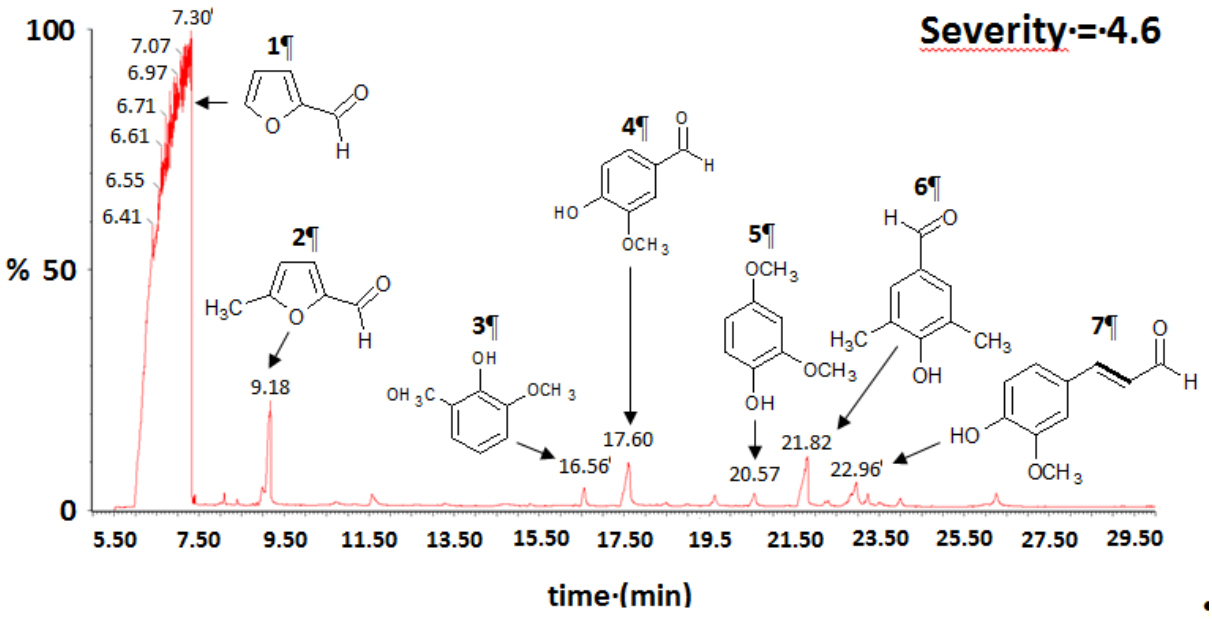

b)

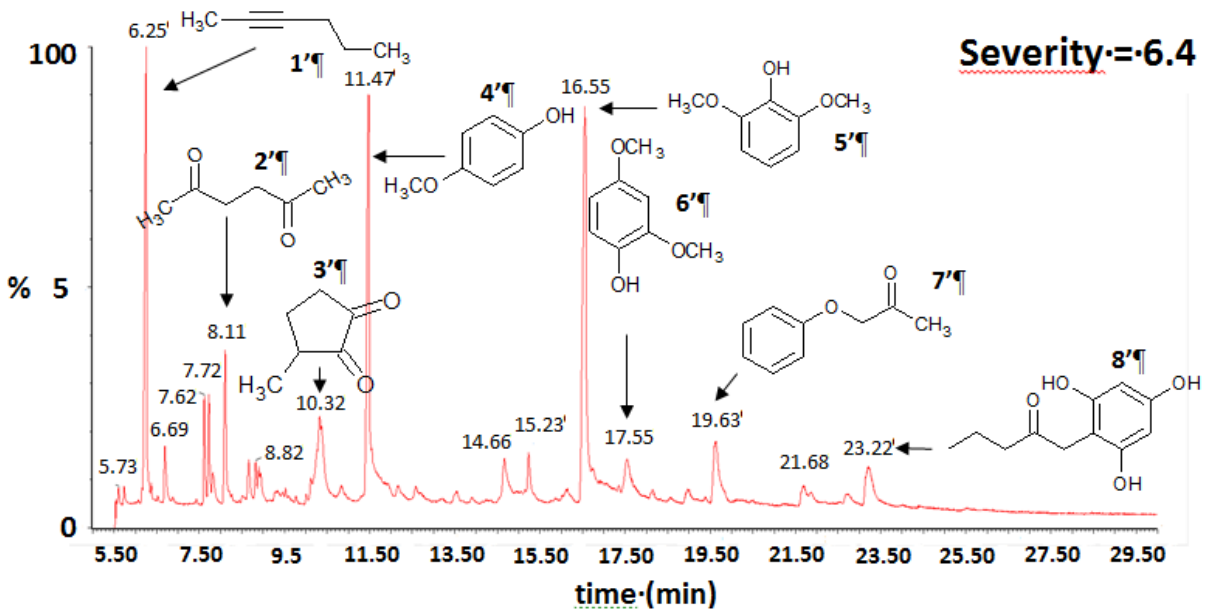

Fig. 7. GC-MS analyses of liquid fractions recovered after HTC: (a) at severity 4.6 (180°C, 3h): Furfural (1), 5-HMF (2), 2,6-dimethoxyphenol (3),vanillin (4), 1-(4-hydroxy-3-methoxyphenyl)-ethanone (5), syringaldehyde (6), and 4-hydroxy-3-methoxycinamaldehyde (7); and (b)at severity 6.4 (200°C, 48h): 2-hexyne (1'), 2,5-Hexanedione (2'), 3-Methyl-1,2-cyclopentanedione (3'), Mequinol (4'), 2,6-dimethoxyphenol (5'), vanillin (6'), 1-(4-hydroxy-3-methoxyphenyl)-2-propanone (7'), and 1-(2,4,6-Trihydrixypenyl)-2-pentanone (8').

Conclusion

A factor combining time and temperature of hydrothermal carbonisation (HTC), the severity factor, was introduced for studying the conversion of olives tones (OS) into high-value products, either liquids or materials. HTC was carried out at temperatures and times ranging from 160°C and 240°C and from 3h and 48 h, respectively. After the treatment, hydrochars and liquid fractions were separated and characterised.

25 different hydrochars were obtained, submitted to thermogravimetric and elemental analyses, and further carbonised at 900°C. The yield to hydrochar varied from 70 to 50% as a function of the HTC severity, and the effect of the latter on OS main components: hemicellulose, cellulose and lignin, was clarified. Hemicelluloses were the most sensitive to HTC, decomposing at severity factors as low as 4, whereas cellulose was degraded at higher severity and lignin in even harsher conditions. Liquid fraction analysis showed that, even at low severity (4.2), lignin started decomposing into vanillin and aldehydes. At severity 4.7, cellulose became accessible and started releasing 5-HMF. At severity $\geq$ 6.4, cellulose totally disappeared. When hydrochars were carbonised, the total yield to carbon varied from 16 to 28%; the resultant carbon materials had high surface areas, as high as 1200 m^2 g^{-1}, and narrow pore size distributions centred on 0.5 nm, suggesting their potential use as cheap carbon molecular sieves. Thus, a preliminary HTC step at the highest severity (i.e., 7.58) before carbonisation did not modify the total yield to carbon when compared with direct pyrolysis, but allowed recovering a valuable liquid fraction and a carbon with a more aromatic structure and a more developed pore texture. The severity factor allowed finding clear tendencies in the production of hydrochars and derived carbons in terms of yield, composition, and surface area, which would have been hardly analysed if the effects of temperature and time had to be considered separately.

References

Álvarez-Murillo A, Román S, Ledesma B, Sabio E (2015) Study of variables in energy densification of olive stone by hydrothermal carbonization. J Anal Appl Pyrolysis 113:307–314. doi: 10.1016/j.jaap.2015.01.031

Anthonia EE, Philip HS (2015) An overview of the applications of furfural and its derivatives. Int J Adv Chem 3:42–47. doi: 10.14419/ijac.v3i2.5048

Benavente V, Calabuig E, Fullana A (2015) Upgrading of moist agro-industrial wastes by hydrothermal carbonization. J Anal Appl Pyrolysis 113:89–98. doi: 10.1016/j.jaap.2014.11.004

Bhatnagar A, Kaczala F, Hogland W, et al (2014) Valorization of solid waste products from olive oil industry as potential adsorbents for water pollution control—a review. Environ Sci Pollut Res 21:268–298. doi: 10.1007/s11356-013-2135-6

Blanco López M., Blanco C., Martínez-Alonso A, Tascón JM. (2002) Composition of gases released during olive stones pyrolysis. J Anal Appl Pyrolysis 65:313–322. doi: 10.1016/S0165-2370(02)00008-6

Bohli T, Ouederni A, Fiol N, Villaescusa I (2015) Evaluation of an activated carbon from olive stones used as an adsorbent for heavy metal removal from aqueous phases. Comptes Rendus Chim 18:88–99. doi: 10.1016/j.crci.2014.05.009

Borrero-López AM, Fierro V, Jeder A, et al (2016) High added-value products from the hydrothermal carbonisation of olive stones. Environ Sci Pollut Res 1–11. doi: 10.1007/s11356-016-7807-6

Braghiroli FL, Fierro V, Izquierdo MT, et al (2015) High surface – Highly N-doped carbons from hydrothermally treated tannin. Ind Crops Prod 66:282–290. doi: 10.1016/j.indcrop.2014.11.022

Díaz I, Rodríguez M, Arnaiz C, et al (2013) Biomass pyrolysis kinetics through thermogravimetric analysis. In: Turunen AK and I (ed) Computer Aided Chemical Engineering. Elsevier, pp 1–6

Do DD, Herrera L, Fan C, et al (2010) The role of accessibility in the characterization of porous solids and their adsorption properties. Adsorption 3. doi: 10.1007/s10450-009-9203-8

Fierro V, Torné-Fernández V, Montané D, Celzard A (2005) Study of the decomposition of kraft lignin impregnated with orthophosphoric acid. Thermochim Acta 433:142–148. doi: 10.1016/j.tca.2005.02.026

Gao P, Zhou Y, Meng F, et al (2016) Preparation and characterization of hydrochar from waste eucalyptus bark by hydrothermal carbonization. Energy 97:238–245. doi: 10.1016/j.energy.2015.12.123

Ghouma I, Jeguirim M, Dorge S, et al (2015) Activated carbon prepared by physical activation of olive stones for the removal of NO2 at ambient temperature. Comptes Rendus Chim 18:63–74. doi: 10.1016/j.crci.2014.05.006

Guo S, Dong X, Wu T, et al (2015) Characteristic evolution of hydrochar from hydrothermal carbonization of corn stalk. J Anal Appl Pyrolysis 116:1–9. doi: 10.1016/j.jaap.2015.10.015

Heilmann SM, Davis HT, Jader LR, et al (2010) Hydrothermal carbonization of microalgae. Biomass Bioenergy 34:875–882. doi: 10.1016/j.biombioe.2010.01.032

Hu B, Wang K, Wu L, et al (2010) Engineering Carbon Materials from the Hydrothermal Carbonization Process of Biomass. Adv Mater 22:813–828. doi: 10.1002/adma.200902812

Ippolito JA, Laird DA, Busscher WJ (2012) Environmental Benefits of Biochar. J Environ Qual 41:967–972. doi: 10.2134/jeq2012.0151

Jagiello J, Ania C, Parra JB, Cook C (2015) Dual gas analysis of microporous carbons using 2D-NLDFT heterogeneous surface model and combined adsorption data of N2 and CO2. Carbon 91:330–337. doi: 10.1016/j.carbon.2015.05.004

Jagiello J, Olivier JP (2013) Carbon slit pore model incorporating surface energetical heterogeneity and geometrical corrugation. Adsorption 19:777–783. doi: 10.1007/s10450-013-9517-4

Jain A, Balasubramanian R, Srinivasan MP (2016) Hydrothermal conversion of biomass waste to activated carbon with high porosity: A review. Chem Eng J 283:789–805. doi: 10.1016/j.cej.2015.08.014

Javad Hosseini S, Aghaie H, Ghaedi M (2012) Preparation and Characterization of Activated Carbon derived from olive stone as adsorbent for Congo Red. J Phys Theor Chem 9:199–208.

Jin F (2014) Application of hydrothermal reactions to biomass conversion. Springer

Kambo HS (2014) Energy Densification of Lignocellulosic Biomass via Hydrothermal Carbonization and Torrefaction. Thesis

Kanetake T, Sasaki M, Goto M (2007) Decomposition of a lignin model compound under hydrothermal conditions. Chem Eng Technol 30:1113–1122. doi: 10.1002/ceat.200700066

Kruse A, Dinjus E (2007) Hot compressed water as reaction medium and reactant: properties and synthesis reactions. J Supercrit Fluids 39:362–380. doi: 10.1016/j.supflu.2006.03.016

Kumagai S, Hirajima T (2014) Effective Utilization of Moso-Bamboo (Phyllostachys heterocycla) with Hot-Compressed Water. In: Jin F (ed) Application of Hydrothermal Reactions to Biomass Conversion. Springer Berlin Heidelberg, Berlin, Heidelberg, pp 155–170

Lowell S, Shields JE, Thomas MA, Thommes M (2012) Characterization of porous solids and powders: surface area, pore size and density. Springer Science & Business Media

Martínez ML, Torres MM, Guzmán CA, Maestri DM (2006) Preparation and characteristics of activated carbon from olive stones and walnut shells. Ind Crops Prod 23:23–28. doi: 10.1016/j.indcrop.2005.03.001

Mohammadi FF, Harrison JT, Czarnota A, Leonard C (2010) Nonabrasive Sensory Exfoliating System.

Mok WS, Antal Jr MJ (1993) Biomass fractionation by hot compressed liquid water. In: Advances in thermochemical biomass conversion. Springer, pp 1572–1582

Montané D (2002) High-temperature dilute-acid hydrolysis of olive stones for furfural production. Biomass Bioenergy 22:295–304. doi: 10.1016/S0961-9534(02)00007-7

Nefzaoui A (1991) Valorisation des sous-produits de l'olivier. In: Fourrages et sous-produits méditerranéens. Tisserand J.-L. and Alibés X., pp 101–108

Nizamuddin S, Baloch HA, Griffin GJ, et al (2017) An overview of effect of process parameters on hydrothermal carbonization of biomass. Renew Sustain Energy Rev 73:1289–1299. doi: 10.1016/j.rser.2016.12.122

Nizamuddin S, Mubarak NM, Tiripathi M, et al (2016) Chemical, dielectric and structural characterization of optimized hydrochar produced from hydrothermal carbonization of palm shell. Fuel 163:88–97. doi: 10.1016/j.fuel.2015.08.057

Oliveira I, Blöhse D, Ramke H-G (2013) Hydrothermal carbonization of agricultural residues. Bioresour Technol 142:138–146. doi: 10.1016/j.biortech.2013.04.125

Overend RP, Chornet E, Gascoigne JA (1987) Fractionation of Lignocellulosics by Steam-Aqueous Pretreatments [and Discussion]. Philos Trans R Soc Lond Math Phys Eng Sci 321:523–536. doi: 10.1098/rsta.1987.0029

Parshetti GK, Kent Hoekman S, Balasubramanian R (2013) Chemical, structural and combustion characteristics of carbonaceous products obtained by hydrothermal carbonization of palm empty fruit bunches. Bioresour Technol 135:683–689. doi: 10.1016/j.biortech.2012.09.042

Pattara C, Cappelletti GM, Cichelli A (2010) Recovery and use of olive stones: commodity, environmental and economic assessment. Renew Sustain Energy Rev 14:1484–1489.

Peterson AA, Vogel F, Lachance RP, et al (2008) Thermochemical biofuel production in hydrothermal media: A review of sub- and supercritical water technologies. Energy Environ Sci 1:32–65. doi: 10.1039/B810100K

Reza MT (2011) Hydrothermal carbonization of lignocellulosic biomass. University of Nevada, Reno

Reza MT, Yang X, Coronella CJ, et al (2016) Hydrothermal Carbonization (HTC) and Pelletization of Two Arid Land Plants Bagasse for Energy Densification. ACS Sustain Chem Eng 4:1106–1114. doi: 10.1021/acssuschemeng.5b01176

Rodríguez G, Lama A, Rodríguez R, et al (2008) Olive stone an attractive source of bioactive and valuable compounds. Bioresour Technol 99:5261–5269. doi: 10.1016/j.biortech.2007.11.027

Rodriguez-Reinoso F, Garrido J, Martin-Martinez JM, et al (1989) The combined use of different approaches in the characterization of microporous carbons. Carbon 27:23–32. doi: 10.1016/0008-6223(89)90153-X

Román S, Valente Nabais JM, Ledesma B, et al (2013) Production of low-cost adsorbents with tunable surface chemistry by conjunction of hydrothermal carbonization and activation processes. Microporous Mesoporous Mater 165:127–133. doi: 10.1016/j.micromeso.2012.08.006

Sabio E, Álvarez-Murillo A, Román S, Ledesma B (2016) Conversion of tomato-peel waste into solid fuel by hydrothermal carbonization: Influence of the processing variables. Waste Manag 47:122–132. doi: 10.1016/j.wasman.2015.04.016

Sánchez-Sánchez A, Martinez de Yuso A, Braghiroli FL, et al (2016) Sugarcane molasses as a pseudocapacitive material for supercapacitors. RSC Adv 6:88826–88836. doi: 10.1039/C6RA16314A

Schaefer S, Fierro V, Izquierdo MT, Celzard A (2016) Assessment of hydrogen storage in activated carbons produced from hydrothermally treated organic materials. Int J Hydrog Energy 41:12146–12156. doi: 10.1016/j.ijhydene.2016.05.086

Sermyagina E, Saari J, Kaikko J, Vakkilainen E (2015) Hydrothermal carbonization of coniferous biomass: Effect of process parameters on mass and energy yields. J Anal Appl Pyrolysis 113:551–556. doi: 10.1016/j.jaap.2015.03.012

Suhas, Carrott PJM, Ribeiro Carrott MML (2007) Lignin – from natural adsorbent to activated carbon: A review. Bioresour Technol 98:2301–2312. doi: 10.1016/j.biortech.2006.08.008

Tan X, Liu S, Liu Y, et al (2017) Biochar as potential sustainable precursors for activated carbon production: Multiple applications in environmental protection and energy storage. Bioresour Technol 227:359–372. doi: 10.1016/j.biortech.2016.12.083

Tejeda-Ricardez J, Vaca-Garcia C, Borredon ME (2003) Design of a Batch Solvolytic Liquefaction Reactor for the Valorization of Residues from the Agricultural Foodstuff. Chem Eng Res Des 81:1066–1070. doi: 10.1205/026387603770866191

Titirici M-M (2013) Sustainable carbon materials from hydrothermal processes. John Wiley & Sons

Ubago-Pérez R, Carrasco-Marín F, Fairén-Jiménez D, Moreno-Castilla C (2006) Granular and monolithic activated carbons from KOH-activation of olive stones. Microporous Mesoporous Mater 92:64–70. doi: 10.1016/j.micromeso.2006.01.002

Volpe M, Fiori L (2017) From olive waste to solid biofuel through hydrothermal carbonisation: The role of temperature and solid load on secondary char formation and hydrochar energy properties. J Anal Appl Pyrolysis 124:63–72. doi: 10.1016/j.jaap.2017.02.022

Wiedner K, Naisse C, Rumpel C, et al (2013) Chemical modification of biomass residues during hydrothermal carbonization – What makes the difference, temperature or feedstock? Org Geochem 54:91–100. doi: 10.1016/j.orggeochem.2012.10.006

Wise L, Murphy M, D'Addieco A. (1946) Chlorite holocellulose, its fractionation and bearing on summative wood analysis and on studies on the hemicelluloses. Pap Trade J 122:35–43.

Yang L, Liu Y, Ruan R, et al (2011) Advances in production of 5-hydroxymethylfurfural from starch. Xiandai HuagongModern Chem Ind 31:32–36.

Zhang B, Huang H-J, Ramaswamy S (2008) Reaction Kinetics of the Hydrothermal Treatment of Lignin. Appl Biochem Biotechnol 147:119–131. doi: 10.1007/s12010-007-8070-6